journal

J. Am. Ceram. Soc., 99 [3] 802–807 (2016)
DOI: 10.1111/jace.14051

Functional Properties of Nd:YAG Polycrystalline Ceramics Processed by High-Pressure Spark Plasma Sintering (HPSPS)

Maxim Sokol, Sergey Kalabukhov, Vladimir Kasiyan, Moshe P. Dariel, and Nachum Frage†,*

Department of Materials Engineering, Ben-Gurion University of the Negev, P.O.B. 653, Beer-Sheva 84105, Israel

High-pressure spark plasma sintering (HPSPS) was employed to fabricate polycrystalline Nd:YAG specimens with desired functional properties. Specimens fabricated under a uniaxial pressure of 300 MPa at 1300°C at a heating rate of 50°C/min and holding time of 60 min displayed submicrometer microstructure and elevated mechanical properties, including resistance to thermal shock. Optical properties (i.e., spectral transmittance, fluorescence emission spectra and fluorescence lifetime) of the HPSPS-processed specimens were close to those obtained with specimens fabricated by conventional sintering procedure. Specifically, remarkable differences in threshold power and laser slope efficiency were found and attributed to the variance in Nd concentration in the specimens tested. The results of this study indicate that the low cost and timesaving HPSPS process allows for the fabrication of polycrystalline Nd:YAG specimens with optical properties suitable for laser applications.

I. Introduction

Nd:YAG-based lasers are used in a wide range of applications in medicine, dentistry, metal manufacturing, and in military hardware.[1] The methods of fabrication and optical properties of transparent polycrystalline ceramics have been widely studied and discussed in the literature.[2–4] Fully dense Nd:YAG ceramics with optical properties identical to those of single-crystal Nd:YAG were fabricated by pressureless sintering at temperatures above 1700°C using silica as a sintering additive.[5,6] Spark plasma sintering (SPS) has also been examined for the fabrication of transparent polycrystalline YAG and Nd:YAG.[7–10] It was reported that starting from YAG and Nd:YAG nanosized powders doped with 0.25 wt% LiF additive, it was possible to obtain ceramics with transparency close to the theoretical limit at significantly lower sintering temperatures (<1400°C).

The successful use of the SPS technique for the fabrication of transparent ceramics entails optimization of SPS processing parameters, namely temperature, heating rate, holding time, and applied pressure. The effects of temperature, heating rate, and holding time on the functional properties of SPS-processed Nd:YAG were discussed in our previous contributions.[7,11,12] Applied pressure in the 63–100 MPa range (see the review of Rubat du Merac et al.[13]) affects neither the transparency nor the mechanical properties of SPS-processed specimens. Nevertheless, in the recent paper of R. Chaim et al.,[14] differences in sintering behavior under pressures of 2 and 100 MPa were clearly detected. Positive effects of pressure applied in the 200–500 MPa range on the transmittance of SPS-processed pure alumina,[15] MgO-doped alumina[16], and MgO (pure and Ca-doped)[17] have also been observed. Recently, we discussed the effects of applied pressure up to 400 MPa on the densification of magnesium aluminate spinel. It was noted that the high-pressure spark plasma sintering (HPSPS) process allowed fabrication of fully dense transparent ceramic with a unique combination of hardness (about 1650 HV) and transparency (82.7% at a wavelength of 550 nm, λ) at a sintering temperature of 1200°C.[18] HPSPS was also recently employed for the fabrication of fully dense non-oxide ceramic, such as tungsten carbide.[19] Such sintering, when performed under an applied pressure of 300 MPa as opposed to 80 MPa, allowed for a lowering of the temperature required for full densification of tungsten carbide by 400°C–500°C. To the best of our knowledge, the effects of applying pressures higher than 100 MPa during SPS consolidation of Nd:YAG powder have not been discussed in the literature. Accordingly, the following report describes the effects of such treatment.

II. Experimental Procedures

(1) Raw Materials and Sintering

Commercial neodymium-doped (1 at.%) yttrium aluminum garnet powder (Nanocerox) was used for the HPSPS experiments. The powder had an average particle size of 50 nm, with a specific surface of 28 m^2/g, and total impurities of 50 ppm. For fabrication of LiF-doped specimens, the Nd:YAG powder was premixed with 0.25 wt% LiF (99.98%, Alfa-Aesar, Heysham, Lancashire, UK). The mixing procedure was reported in our previous contributions.[7,12]

Consolidation experiments were performed using an SPS apparatus (FCT Systems, Rauensein, Germany). The SPS parameters varied as follows: Sintering temperature from 1200°C–1300°C, heating rate from 2°C/min–100°C/min, holding time at the sintering temperature from 2–90 min, and applied pressure from 200–400 MPa. An example of the SPS regimes for sintering temperature 1300°C, heating rate of 50°C/min, holding time 20 min, and applied pressure 300 MPa together with relative punch displacement (RPD) curve is presented in Fig. 1. To achieve high pressure during the sintering process, a hybrid tool composed of silicon carbide and graphite was used. The precise description of the tooling set up was presented elsewhere.[18]

(2) Mechanical Properties and Microstructural Characterization

Samples were mounded and polished to an optical level. The final thickness after polishing was about 1 mm. Microstructure was analyzed by using a high-resolution scanning electron microscope (JSM-7400; JEOL, Tokyo, Japan). For microstructure characterization, the samples were thermally etched at 1350°C for 1–2 min under ambient atmosphere. Grain size distribution was determined from SEM micrographs using Thixomet image analysis software.[20,21] The density of the sintered specimens was determined by the Archimedes technique. Bending strength was determined by

H. Chan—contributing editor

Manuscript No. 37161. Received July 6, 2015; approved November 5, 2015.
*Member, The American Ceramic Society.
†Author to whom correspondence should be addressed. e-mail: nfrage@bgu.ac.il

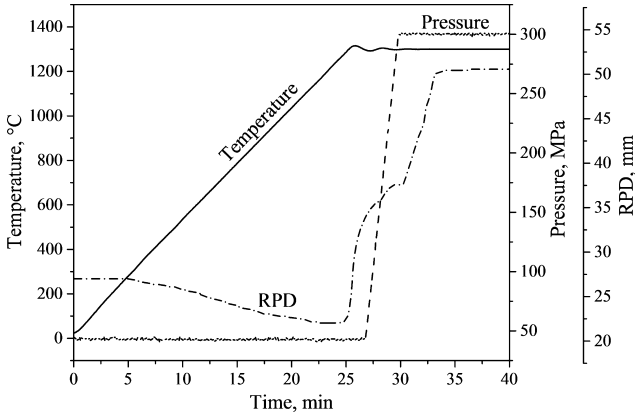

Fig. 1. The temperature and pressure regimes together with the relative punch displacement during the course of the spark plasma sintering (SPS) treatment.

a three-point test using a LRXPlus tensile tester (Lloyd Instruments, Fareham, U.K.). Hardness measurements were obtained under a 2000 g load using a Buehler Micromet 2010 apparatus. The elastic modulus was determined by the "pulse echo" method. Thermal conductivity was measured in a temperature region spanning from room temperature to 125°C by the flash diffusivity method (LFA 457, NETZSCH GmbH, Selb, Bavaria, Germany). The thermal expansion coefficient was measured under a stream of argon at a heating rate of 2°C/min using a Unitherm 1252 dilatometer (Thermal Expansion System, Anter). Thermal shock resistance was calculated using the expression:

$$R_T = \frac{k\sigma(1-\nu)}{\alpha E} \quad (1)$$

where k is thermal conductivity in W/mk, σ is strength in Pa, ν is the passion ratio, α is the thermal expansion coefficient in $°C^{-1}$, and E is the elastic modulus in Pa.

(3) Optical Properties Characterization

A number of spectroscopic properties are of prime importance in considering a material as a laser cavity material. The following relevant properties were tested in the present manuscript: (i) spectral transmittance or absorption that characterizes the opacity of the material to the pumped and emitted radiations; (ii) fluorescence emission spectra, which relate to the gain coefficient and saturation fluence; (iii) fluorescence lifetime, which determines stored energy density; and (iv) laser performance.

Spectral transmittance was measured in the 400–1100 nm range. An incandescent 250 W tungsten halogen lamp served as light source. The light beam was chopped at 140 Hz and a monochromator (HORIBA Ltd., Kyoto, Japan) with 1.2 nm/mm spectral dispersion provided spectral separation. Signals were measured with a Si photodetector and amplified by a lock-in amplifier (Signal Recovery, 1265 DSP).

Emission spectra were measured at room temperature using an 808 nm diode laser (CNI Optoelectronics Tech, Changchun, China) as excitation source. The florescence signal was treated with the same method as described for the spectral transmittance measurements, above.

Neodymium fluorescence lifetime was determined using a nitrogen laser (Stanford Research Systems, Sunnyvale, CA) by exciting the sample at a λ equal to 337.1 nm with 3.5 nsec pulse duration. Emission was collected with a silicon-amplified detector equipped with a 1064 nm wavelength filter (Thorlabs).

Laser performance and lasing slope efficiency were evaluated using an optical resonator pumped by an 808 nm laser diode. The laser resonator was based on a flat high reflection mirror containing a 1 m convex mirror with 96% reflection at a 1064 nm wavelength. The sample was oriented at Brewster's angle from the optical axis of the resonator. The laser emission was measured by a powermeter (Coherent FieldMax-TO laser power-meter). No antireflection coating was applied to the samples.

A commercial polycrystalline Nd:YAG (1 at.%) ceramic (1 mm thickness) fabricated by conventional sintering procedure (Photonik Singapore), marked below as reference sample, was also examined. The obtained properties were compared to those of the HPSPS-processed specimen.

III. Results and Discussion

Specimens sintered at temperatures below 1300°C, regardless of the pressure in 200–400 MPa range applied, were translucent (level of transparency of about 50%) only due to residual porosity. Thus, only specimens sintered at 1300°C with various heating rates, holding times, and applied pressures are discussed below.

It was reported that optical transparency of SPS-processed (under pressure of 50–100 MPa) polycrystalline ceramics depended on the heating rate, with better transparency being achieved at a heating rate of 2–5°C/min.[12,22] The same results were obtained in this study for nondoped specimens, with transmittance increasing with a decrease in heating rate (Fig. 2). Nevertheless, the transparency of the nondoped specimens was relatively low. The transparency of LiF-doped specimens was significantly higher and monotonically increased with the heating rate. Maximal transparency was achieved with a heating rate of about 50°C/min.

Prolonged sintering duration led to decreased transparency for both doped and nondoped specimens (Fig. 3), likely due to the formation of a large number of oxygen vacancies and color centers under the reducing atmosphere within the SPS apparatus.[22]

Increasing applied pressure from 200 to 300 MPa led to a significant increase in transparency (Fig. 4), whereas transparency of samples sintered under 400 MPa pressure was almost the same as samples sintered under 300 MPa pressure.

Based on these results, we concluded that the optimal parameters of HPSPS of LiF-doped Nd:YAG powder to be a sintering temperature of 1300°C, a holding time of 60 min and an applied pressure of 300 MPa.

SEM images of the microstructure of doped and nondoped HPSPS-processed specimens, along with microstructural images of specimens fabricated under 60 MPa pressure

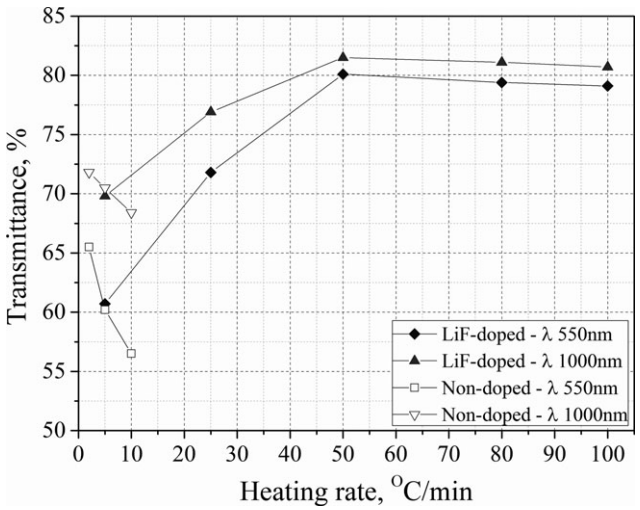

Fig. 2. The effect of heating rates on the transparency of Nd:YAG processed at 1300°C under 300 MPa for 60 min.

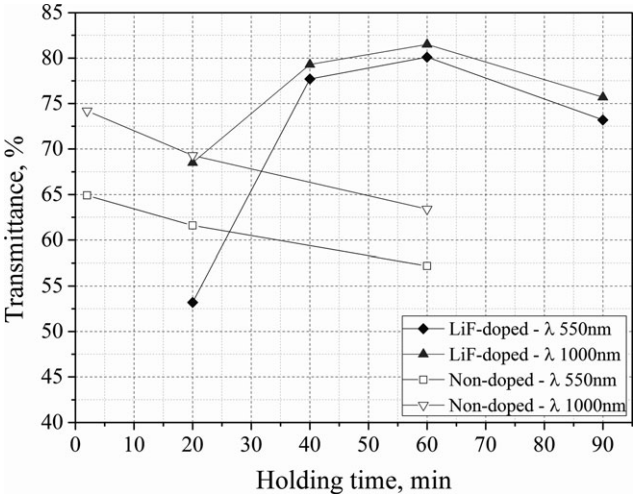

Fig. 3. The effect of holding time on the transparency of Nd:YAG processed by high-pressure spark plasma sintering (HPSPS) (applied pressure 300 MPa, sintering temperature 1300°C, and heating rate of 50°C/min).

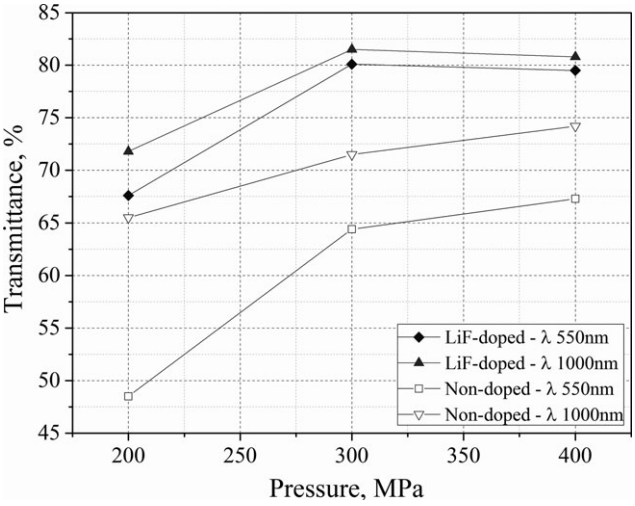

Fig. 4. The effect of pressure on the transparency of Nd:YAG processed by high-pressure spark plasma sintering (HPSPS) (sintering temperature 1300°C, holding time 60 min, and heating rate of 50°C/min).

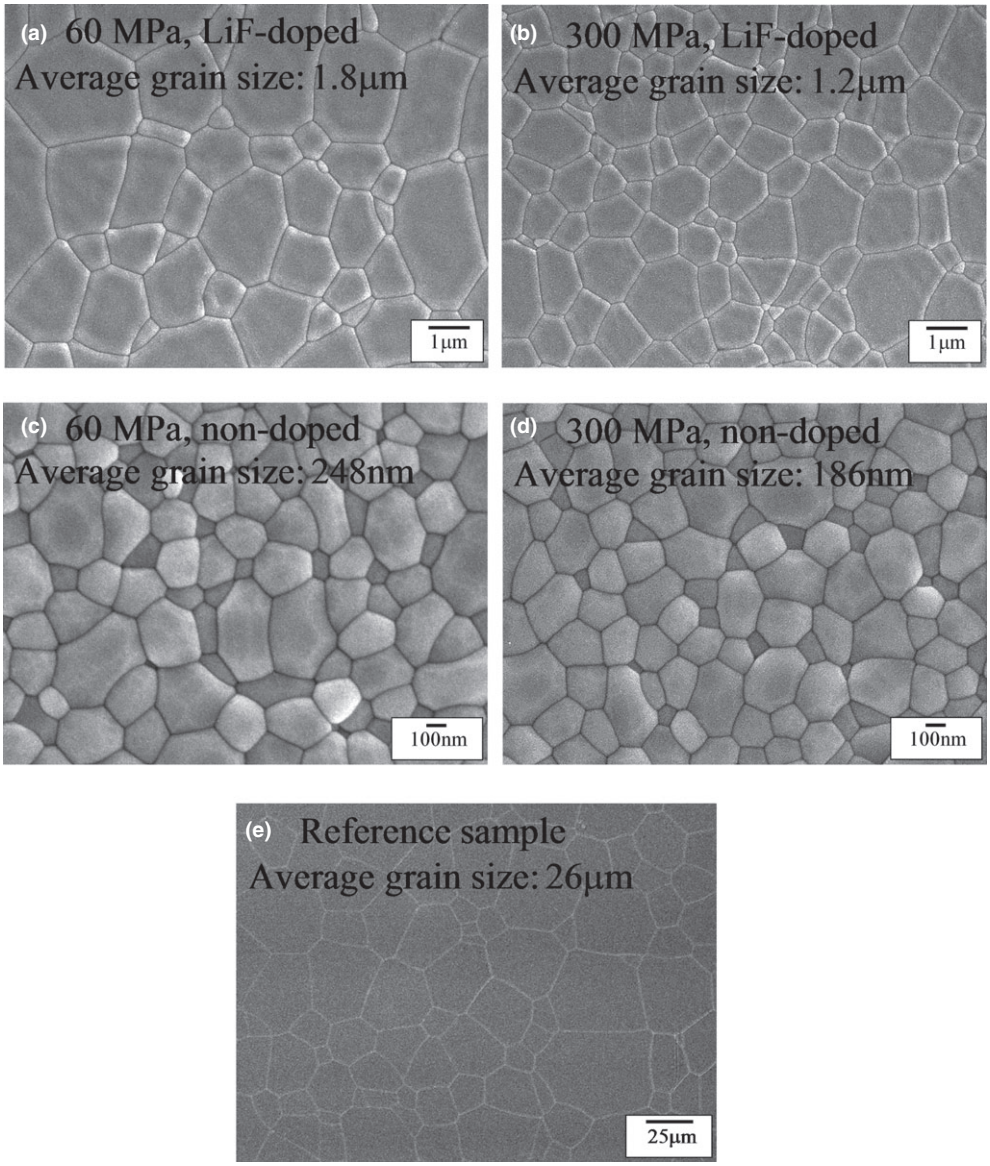

Fig. 5. High-resolution scanning electron microscope (SEM) images of the microstructure of: (a) 60 MPa LiF-doped, (b) 300 MPa LiF-doped, (c) 60 MPa nondoped, (d) 300 MPa nondoped samples, and (e) a sample prepared by the conventional sintering procedure (reference sample).

at 1400°C and by conventional sintering procedure (reference sample) are presented in Fig. 5. Both doped and non-doped HPSPS-processed specimens displayed fine microstructure, with grains sized smaller than those detected in specimens fabricated under 60 MPa pressure. The average grain size of the reference sample was significantly larger, namely 26 vs 1.2 μm. The mechanical properties of the specimens (Table I) reflect the microstructural features.

The specimens fabricated under 300 MPa pressure had finer microstructure and displayed higher bending strength, hardness, and resistance to thermal shock. The reference sample fabricated by the conventional sintering procedure at high temperature displayed coarse microstructure and much lower mechanical properties.

Transmittance spectra of specimens fabricated under optimal conditions, along with the reference sample, are presented in Fig. 6. Absorption in the 780–840 wavelength region was calculated using Eq. (2) and is shown in Fig. 7.

The absorption peaks corresponded to the Nd dopant and were similar for both samples. Transparency of the reference sample was slightly higher and the adsorption was directly related to the transmittance (Fig. 6). However, the difference in real absorption coefficients calculated by taking into account the background (internal losses) of the samples [Fig. 7(b)] could be attributed to variances in the Nd ion concentration.

The fluorescence spectra of the HPSPS-processed and reference specimens are presented in Fig. 8(a). The samples showed a consistent fluorescence spectrum profile. The line shape for the most intense transition could be accurately fitted by a Gaussian function with a FWHM of 0.946 and 1.005 nm for the HPSPS sample and for the reference ceramic, respectively. The measured fluorescence decay times [Fig. 8(b)] were slightly different and indicated that the specimens did not share the same Nd concentration.[23]

Table I. Mechanical Properties of Polycrystalline Nd:YAG

Sample	Bending strength, MPa (±12)	Vickers hardness, HV (±15)	Shear modulus, GPa (±1)	Young modulus, GPa (±2)	Thermal shock resistance, Wm^{-1}
Single crystal	200	1320	113	284	761
60 MPa, undoped	420	1570	114	285	1582
60 MPa, doped	310	1460	114	286	1294
300 MPa, undoped	510	1610	114	285	1859
300 MPa, doped	350	1510	114	286	1448
Reference sample	300	1100	114	285	1084

The laser oscillation characteristics (slope efficiency, SE, and threshold powder, P_{th}) of the specimen sintered by the HPSPS method relative to those of the commercial sample sintered by conventional method are presented in Fig. 9. The absorbed power was calculated by$P_{abs} = P_{pump}\int_0^L \exp(-\alpha_{abs}x)dx$, where P_{pump} is pumping power, α_{abs} is the absorption coefficient at λ = 808 nm, and x is the path length of the beam which varies from 0 up to the sample thickness, L.

According to the measurements of the two samples, differences in SE and P_{th} exist. Taking into account that the reference sample displayed slightly higher transmittance and consequently, a smaller absorption coefficient, these differences could be attributed to variances in the Nd concentration of the investigated samples. The true concentration of

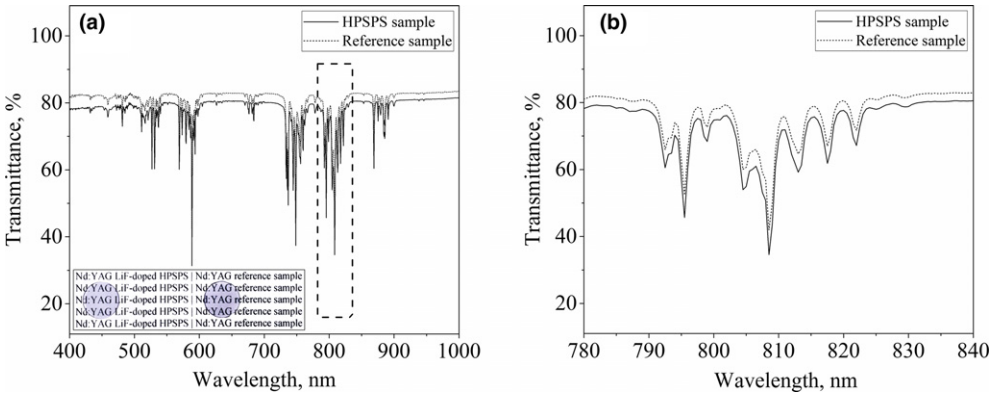

Fig. 6. (a) Spectral transmittance of Nd:YAG ceramics, (b) transmittance in the 780–840 nm wavelength range. Photos of the mirror-polished Nd:YAG samples are presented in the insert.

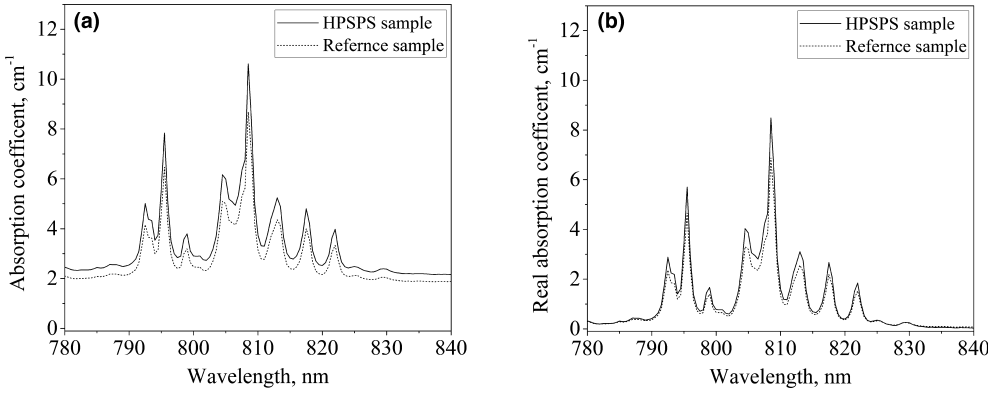

Fig. 7. (a) Absorption coefficent of Nd:YAG ceramics, (b) real absorption coefficent in the 780–40 nm wavelength range.

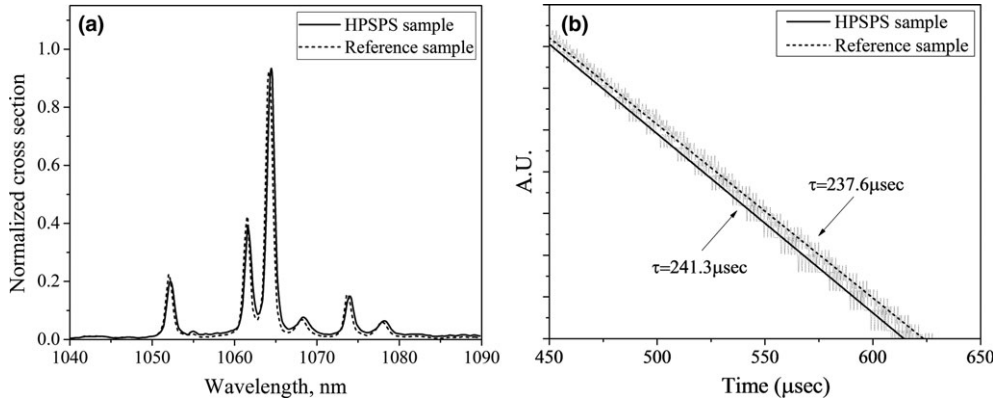

Fig. 8. (a) Emission spectra of Nd:YAG ceramics at room temperature in the 1040–1090 nm range, (b) normalized decay profiles of the emissions.

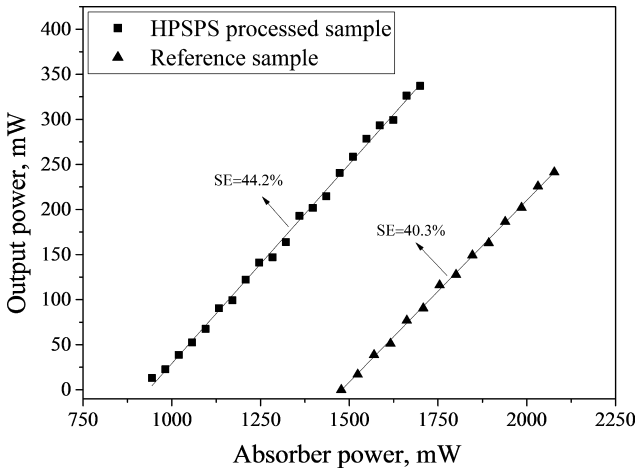

Fig. 9. Laser oscillation characteristics of Nd:YAG ceramics.

Nd can be estimated from the lifetime (τ) measurements presented above (Fig. 8 insert) and from the correlation [Eq. (2)] between Nd concentration (N_{Nd}, at.%) and τ obtained from reported experimental data.[24]

$$\tau = 259.281 - 4.769N_{Nd} - 29.417N_{Nd}^2 + 5.348N_{Nd}^3 \qquad (2)$$

Calculated Nd concentrations were equal to 0.863 and 0.783 at.% for the SPS-processed and reference samples, respectively. In addition, the ratio of Nd concentration in the investigated samples could be estimated using the relation $\alpha_{abs} = N\sigma_{Nd}$, where N is the number of Nd ions and σ_{Nd} is the Nd absorption cross section. Assuming that σ_{Nd} is constant and using α_{abs} values (Fig. 7), the real Nd concentration in the HPSPS-processed sample was calculated to be about 20% higher than in the reference sample. The estimated values of the Nd concentrations support our suggestion regarding differences in the laser performance of the investigated samples.

The results of this study indicate that the low cost and timesaving HPSPS process allows for the fabrication of polycrystalline Nd:YAG specimens with optical properties suitable for laser applications.

IV. Conclusions

The effects of HPSPS parameters on microstructure, and mechanical and optical properties were investigated. It was established that optimal HPSPS parameters for the sintering of LiF-doped Nd:YAG powder were a heating rate of 50°C/min, a sintering temperature of 1300°C, a holding time of 60 min, and an applied pressure of 300 MPa. Fully dense polycrystalline Nd:YAG specimens with fine microstructure and elevated mechanical properties were fabricated and their optical properties were tested. Optical properties, such as spectral transmittance and fluorescence emission spectra, of the HPSPS-processed specimens were close to those of specimens fabricated by conventional sintering, although differences were found in slope efficiency and threshold power. These differences were attributed to the difference in the true Nd concentration in the investigated samples. Effective laser oscillation of the HPSPS-processed sample, comparable to that of the same specimen fabricated by conventional sintering, was successfully achieved for the first time using a low cost and timesaving approach.

References

[1]A. Ikesue and Y. L. Aung, "Ceramic Laser Materials," *Nat. Photonics*, **2** [12] 721–7 (2008).
[2]A. Ikesue and K. Yoshida, "Influence of Pore Volume on Laser Performance of Nd:YAG Ceramics," *J. Mater. Sci.*, **34** [6] 1189–95 (1999).
[3]R. Fedyk, et al., "Method of Preparation and Structural Properties of Transparent YAG Nanoceramics," *Opt. Mater.*, **29** [10] 1252–7 (2007).
[4]W. Liu, et al., "Influence of Heating Rate on Optical Properties of Nd:YAG Laser Ceramic," *Ceram. Int.*, **36** [7] 2197–201 (2010).
[5]S. Kochawattana, et al., "Sintering and Grain Growth in SiO_2 Doped Nd:YAG," *J. Eur. Ceram. Soc.*, **28** [7] 1527–34 (2008).
[6]X. Li, "Fabrication of Transparent Yttrium Aluminum Garnet Ceramic," *J. Phys: Conf. Ser.*, **152** [1] 012079 (2009).
[7]N. Frage, S. Kalabukhov, N. Sverdlov, V. Ezersky, and M. P. Dariel, "Densification of Transparent Yttrium Aluminum Garnet (YAG) by SPS Processing," *J. Eur. Ceram. Soc.*, **30** [16] 3331–7 (2010).
[8]R. Chaim, M. Kalina, and J. Z. Shen, "Transparent Yttrium Aluminum Garnet (YAG) Ceramics by Spark Plasma Sintering," *J. Eur. Ceram. Soc.*, **27** [11] 3331–7 (2007).
[9]R. Chaim, R. Marder, and C. Estournès, "Optically Transparent Ceramics by Spark Plasma Sintering of Oxide Nanoparticles," *Scr. Mater.*, **63** [2] 211–4 (2010).
[10]G. Spina, G. Bonnefont, P. Palmero, G. Fantozzi, J. Chevalier, and L. Montanaro, "Transparent YAG Obtained by Spark Plasma Sintering of co-Precipitated Powder. Influence of Dispersion Route and Sintering Parameters on Optical and Microstructural Characteristics," *J. Eur. Ceram. Soc.*, **32** [11] 2957–64 (2012).
[11]M. Sokol, S. Kalabukhov, V. Kasiyan, A. Rothman, M. P. Dariel, and N. Frage, "Mechanical, Thermal and Optical Properties of the SPS-Processed Polycrystalline Nd:YAG," *Opt. Mater.*, **38** [0] 204–10 (2014).
[12]N. Frage, S. Kalabukhov, N. Sverdlov, V. Kasiyan, A. Rothman, and M. P. Dariel, "Effect of the Spark Plasma Sintering (SPS) Parameters and LiF Doping on the Mechanical Properties and the Transparency of Polycrystalline Nd-YAG," *Ceram. Int.*, **38** [7] 5513–9 (2012).
[13]M. Rubat du Merac, H. Kleebe, M. M. Müller, and I. E. Reimanis, "Fifty Years of Research and Development Coming to Fruition; Unraveling the Complex Interactions During Processing of Transparent Magnesium Aluminate ($MgAl_2O_4$) Spinel," *J. Am. Ceram. Soc.*, **96** [11] 3341–65 (2013).
[14]R. Marder, C. Estournès, G. Chevallier, and R. Chaim, "Spark and Plasma in Spark Plasma Sintering of Rigid Ceramic Nanoparticles: A Model System of YAG," *J. Eur. Ceram. Soc.*, **35** [1] 211–8 (2015).
[15]S. Grasso, H. Yoshida, H. Porwal, Y. Sakka, and M. Reece, "Highly Transparent α-Alumina Obtained by low Cost High Pressure SPS," *Ceram. Int.*, **39** [3] 3243–8 (2013).

[16]S. Grasso, B. Kim, C. Hu, G. Maizza, and Y. Sakka, "Highly Transparent Pure Alumina Fabricated by High-Pressure Spark Plasma Sintering," *J. Am. Ceram. Soc.*, **93** [9] 2460–2 (2010).
[17]T. B. Tran, S. Hayun, A. Navrotsky, and R. H. R. Castro, "Transparent Nanocrystalline Pure and Ca-Doped MgO by Spark Plasma Sintering of Anhydrous Nanoparticles," *J. Am. Ceram. Soc.*, **95** [4] 1185–8 (2012).
[18]M. Sokol, S. Kalabukhov, M. P. Dariel, and N. Frage, "High-Pressure Spark Plasma Sintering (SPS) of Transparent Polycrystalline Magnesium Aluminate Spinel (PMAS)," *J. Eur. Ceram. Soc.*, **34** [16] 4305–10 (2014).
[19]S. Grasso, J. Poetschke, V. Richter, G. Maizza, Y. Sakka, and M. J. Reece, "Low-Temperature Spark Plasma Sintering of Pure Nano WC Powder," *J. Am. Ceram. Soc.*, **96** [6] 1702–5 (2013).
[20]A. Kazakov, N. Luong, E. Kazakova, and E. Zorina, "Thixomet Image Analyzer for Characterization of 2D and 3D Materials Structure," *Microstr. Sc.*, **27**, 133–42 (1999).
[21]A. A. Kazakov and N. H. Luong, "Characterization of Semisolid Materials Structure," *Mater. Charact.*, **46** [2–3] 155–61 (2001).
[22]K. Morita, B. Kim, H. Yoshida, K. Hiraga, and Y. Sakka, "Influence of Spark Plasma Sintering (SPS) Conditions on Transmission of MgAl2O4 Spinel," *J. Am. Ceram. Soc.*, **98** [2] 378–85 (2015).
[23]A. Ikesue, K. Kamata, and K. Yoshida, "Effects of Neodymium Concentration on Optical Characteristics of Polycrystalline Nd:YAG Laser Materials," *J. Am. Ceram. Soc.*, **79** [7] 1921–6 (1996).
[24]J. Lu, et al., "Potential of Ceramic YAG Lasers," *Laser Physics-Lawrence*, **11** [10] 1053–7 (2001). □